Available online at www.sciencedirect.com
ScienceDirect
Precambrian Research 162 (2008) 86–101
Precambrian Research
www.elsevier.com/locate/precamres

Transpressional tectonics during the emplacement of Pasupugallu Gabbro Pluton, Western margin of Eastern Ghats Mobile Belt, India: Evidence from AMS fabrics

J. Nagaraju [a], T.R.K. Chetty [a,*], G.S. Vara Prasad [a], S.K. Patil [b]

[a] *National Geophysical Research Institute, Hyderabad 7, India*
[b] *Indian Institute of Geomagnetism, Alibag, India*

Received 12 July 2006; received in revised form 2 March 2007; accepted 4 July 2007

Abstract

The Pasupugallu Gabbro–Anorthosite Pluton intruded the transition zone between the Mesoproterozoic Eastern Ghats granulites and the Meso- to Paleoproterozoic amphibolites and migmatitic gneisses of East Dharwar Craton, southern India. The pluton is bound by shear zones at its entire eastern, northern and southwestern margins. The objective of this work is to study the internal fabric of the pluton to understand the tectonic setting during its emplacement, essentially by means of Anisotropy of Magnetic Susceptibility (AMS). A total number of 107 samples have been subjected to AMS and IRM studies. The magnetic fabric is principally ferromagnetic in origin as the magnetic susceptibility values are $>10^{-3}$ SI, which is further supported by IRM studies. The magnetic fabrics correspond well with the field measurements and petrographic studies. They show two lobes in both the northern and southern parts which display concentric inward dipping helicoidal foliation trajectories with interlayered steep and gently dipping domains. The magnetic lineation pattern suggests that the magma might have ascended through the central lobes and extended towards outer margins, particularly to the west. The constrictional strains occur at the eastern margin while flattening strains mark the western margin. AMS studies together with our field structural observations suggest that the magma has been emplaced into a chamber (dilational jog) induced by crustal-scale dextral transpressional tectonic regime, probably during the onset of Grenvilian event.

Keywords: Anisotropy of magnetic susceptibility; Gabbro Pluton; Eastern ghats; Magma emplacement; Transpression

1. Introduction

Study of internal fabrics of plutonic complexes within the orogenic belts is one of the critical factors in constraining the regional tectonics, since the magmatism can be associated with both compressional and extensional phases of an orogeny (Brown and Solar, 1998; Saint Blanquat et al., 1998). The plutonic fabrics reflect the interplay between tectonic stresses and internal magmatic dynamics that record the ‘snap-shot’ of prevailing tectono-thermal conditions during the emplacement. Layering in basic intrusives can be caused by magmatic and subsolidus to metamorphic processes that can be distinguished by petrofabric studies. Several mechanisms like gravitational accumulation, fractional crystallization, convection currents and magmatic sub-solidus shearing, etc. have been ascribed for the generation of magmatic layering (Cawthorn, 1996). But, heterogeneity in the intensity of layering and absence of well-developed mineral lineations hinder comprehensive structural study of many layered mafic intrusions. Therefore, Anisotropy of Magnetic Susceptibility (AMS) studies have become crucial in studying the nature of isotropic rocks as they can well characterize the nature of magma streams (Ellwood and Whitney, 1980; Borradaile, 1988).

AMS is a rapid and non-destructive measurement technique to detect the subtle fabrics in igneous rocks (Archanjo et al., 1994; Borradaile and Henry, 1997). It is the measurement of anisotropy of the acquired magnetization (M) of the material, when it is subjected to an external field (H), i.e. $M_i = K_{ij}H_j$ (Tarling and Hrouda, 1993). This susceptibility tensor K_{ij} is geometrically represented by a triaxial ellipsoid whose principal magnitudes and orientations are $K_1 \geq K_2 \geq K_3$. The long axis of the AMS ellipsoid (K_1) represents magnetic lineation and the short axis (K_3) is normal to the magnetic foliation. It has

* Corresponding author. Tel.: +91 40 23434611; fax: +91 40 23434651.
E-mail address: chettytrk@yahoo.co.in (T.R.K. Chetty).

0301-9268/$ – see front matter © 2007 Elsevier B.V. All rights reserved.
doi:10.1016/j.precamres.2007.07.025

been demonstrated that magmatic flow aligns minerals parallel to the magnetic foliation plane (K_1–K_2) (Khan, 1962; King, 1966; Wing-Fatt and Stacey, 1966; Symons, 1967). AMS fabrics may therefore be related to emplacement (e.g., diapiric inflation) in the case of undeformed plutons; otherwise they simply preserve the record of last deformational event (Borradaile and Henry, 1997).

AMS studies have been successfully tested in the study of numerous plutonic complexes all over the world (e.g., Borradaile et al., 1998; Cowan, 1999; Bolle et al., 2000; Asrat et al., 2003; Parada et al., 2005). In the present study, AMS fabrics are particularly helpful considering (a) the absence of post-magmatic deformational evidences and poorly developed mineral lineation, and (b) the association of ferromagnetic minerals (oxides) along with the paramagnetic ferromagnesian silicate layering. In this contribution, we present our new results of AMS, field and petrographic data of the Pasupugallu layered gabbro-anorthosite pluton located at the interface of a mobile belt and the craton to better understand its emplacement history and tectonic setting.

2. Regional geological setting

The Pasupugallu Gabbro Pluton (PGP) is a part of the Prakasam Igneous Province (Prasada Rao et al., 1988; Leelanandam, 1989) that hosts a colony of numerous alkaline, mafic–ultramafic–anorthosite and granitic plutons. This province (∼1450–1100 Ma) forms a NE–SW trending linear belt straddling the transition zone between the Mesoproterozoic Eastern Ghats Mobile Belt (EGMB) and the Paleoproterozoic East Dharwar craton, southeastern Indian shield (inset, Fig. 1). This transition zone has also been described as a Terrane Boundary Shear Zone (TBSZ, Nagaraju and Chetty, 2005) as well as a cryptic suture zone (Leelanandam, 1990; Singh and Mishra, 2002). These elliptical to linear plutons of the Prakasam Igneous Province are preferentially emplaced in an en-echelon fashion along the deep fault systems within the TBSZ (Fig. 1A). Several workers have invoked collision tectonics involving the transpressional tectonic regime between the craton and the EGMB (e.g. Chetty and Murthy, 1994; Singh and Mishra, 2002; Saha, 2004). Recently, Leelanandam et al. (2006) have described the

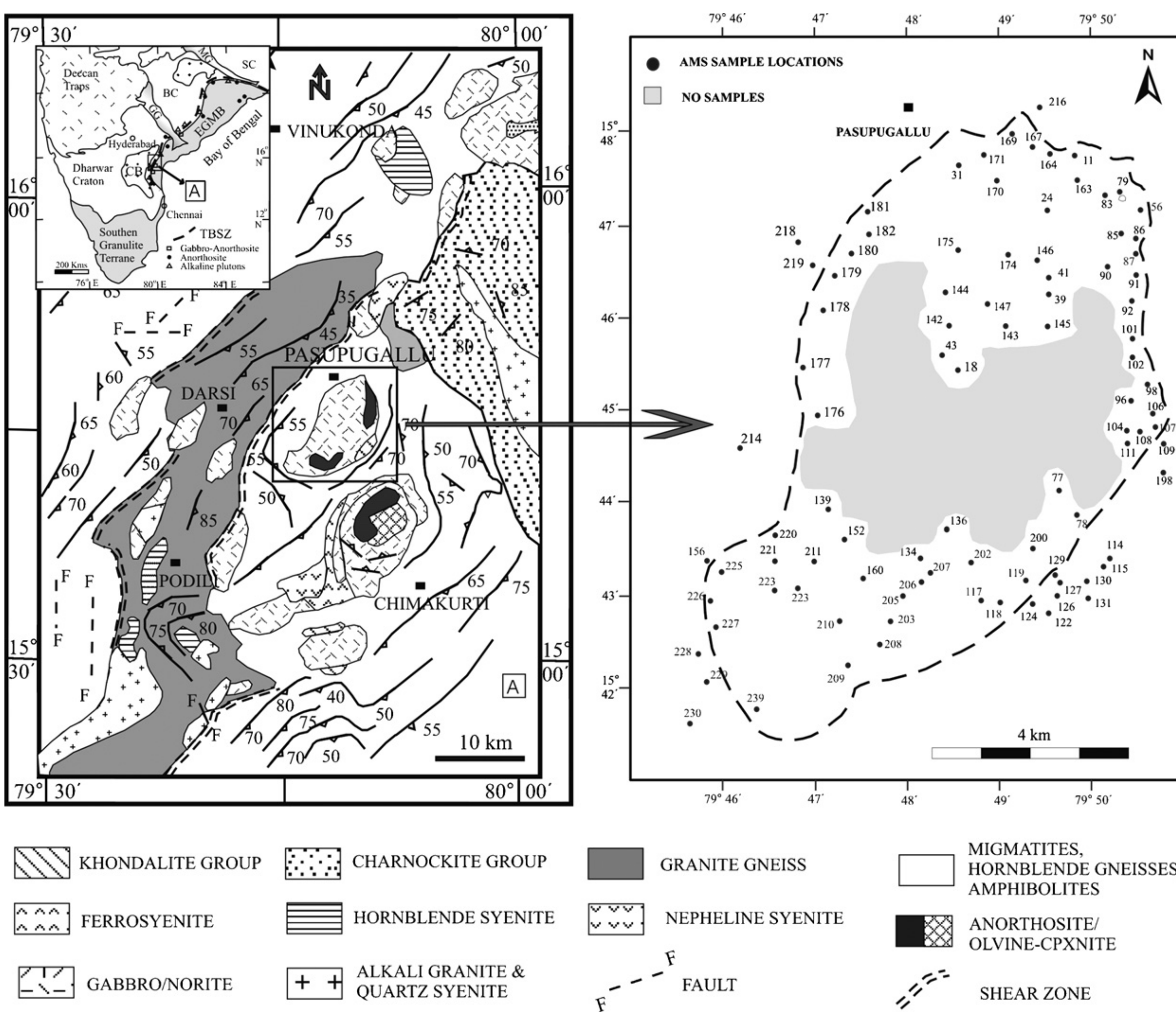

Fig. 1. (A) Regional geological map showing the distribution of various alkaline, mafic and granitic plutons in the transition zone between the Eastern Ghats high-grade gneisses and Archaean Dharwar schists and migmatites (modified after Prasad Rao et al., 1988). The inset map shows the geological setting of the igneous complexes and study area in southern India. Abbreviations used: CB-Cuddapah basin, BC-Bastar craton, SC-Singhbhum craton, EGMB-Eastern Ghats Mobile Belt, TBSZ-Terrane Boundary Shear Zone. (B) The map of Pasupugallu gabbro pluton showing the locations of the samples collected for AMS studies.

alkaline plutons in this province as Deformed Alkaline Rocks and Carbonatites (DARCs) and considered the transition zone as a Proterozoic fossil plate boundary.

2.1. The transition zone

The transition zone or TBSZ is a ~60 km wide linear zone trending N–S to NNE–SSW, marked by boundary shear zones separating the Nellore–Khammam schist belt to the west and the charnockitic rocks of the EGMB to the east (Fig. 1A). The strain has been partitioned heterogeneously along the minor en-echelon shear zones within the transition zone (Ramam and Murthy, 1997; unpublished data of the authors), which encircle these plutonic complexes. The host rocks include migmatised hornblende schists, amphibolites, granitic gneisses, leptynites and enderbitic charnockites. They display N–S to NE–SW trending gneissic foliation with steep easterly dips. The radiometric ages are scarce to constrain the major tectono-magmatic episodes in the region, but the tholeiitic mafic–ultramafic magmatism appears to post-date the deformed and metamorphosed alkaline magmatic bodies.

2.2. Geology of Pasupugallu Pluton

The Pasupugallu Gabbro Pluton (Fig. 2), an elliptical body (8 × 13 km) with NE-SW trending long axis, intruded the tran-

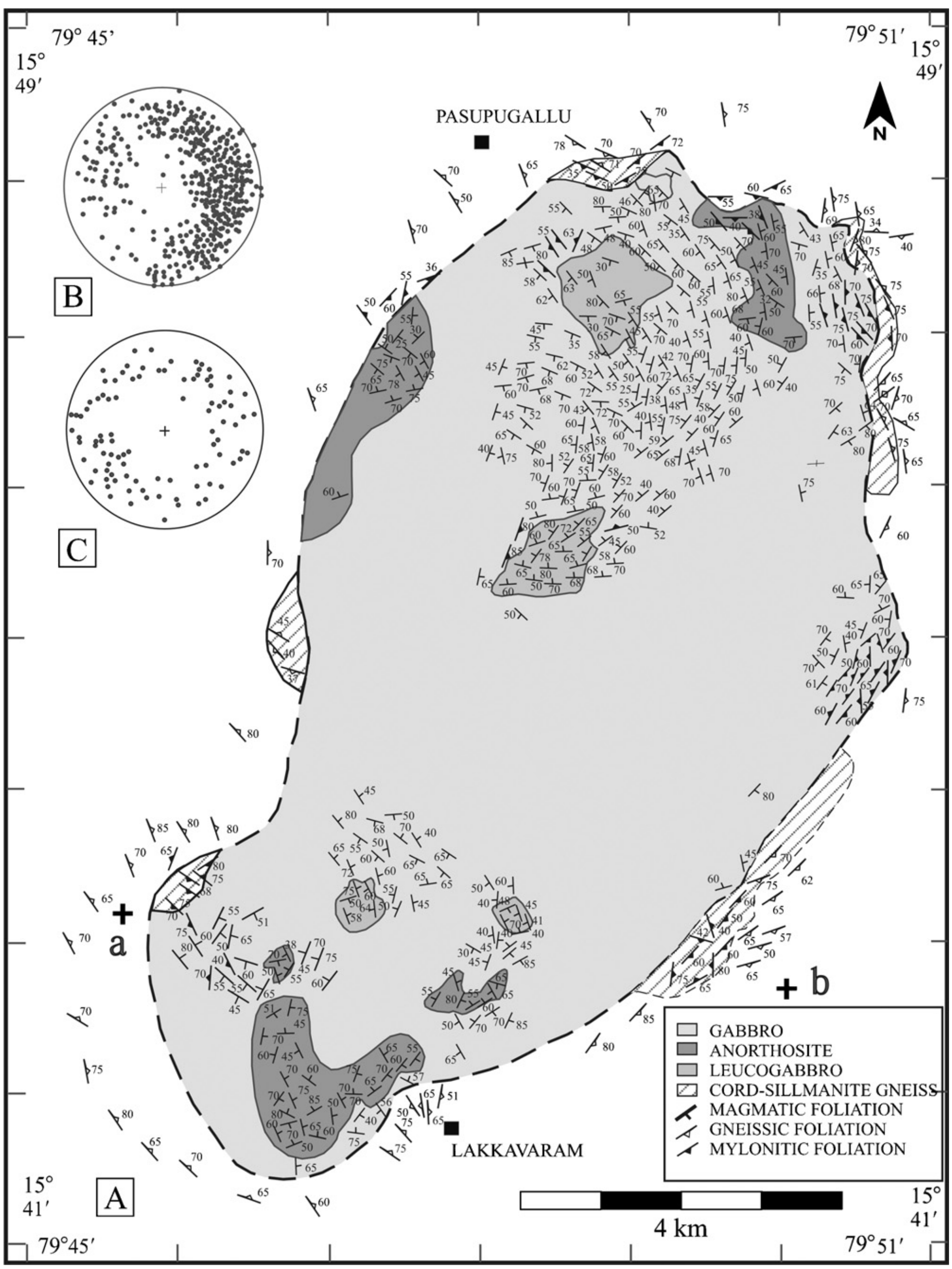

Fig. 2. (A) The geological and structural map of Pasupugallu gabbro pluton. Equal area stereoplot (lower hemisphere) of poles to magmatic foliations in the northern half of the pluton (B) and southern half of the pluton (C).

sition zone comprising amphibolite–granulite facies rocks of Ongole domain (Dobmeier and Raith, 2003). The pluton consists essentially of gabbro and anorthosite with leucogabbro-norite as the subordinate unit. All the lithologies are traversed by dolerite dykes, mostly in N–S to NE–SW directions with a few pegmatite and syenite dikes. The gabbroic rocks display well-developed igneous layering, manifested by systematic changes in the phase proportions and rhythmic modal layering of minerals. The mineral layering exposes centimeter to meter scale alternate trough (pyroxene–biotite–magnetite rich cumulates) and ridge bands (plagioclase rich portions). The outcrops are scanty and are not much exposed in the central parts of the pluton. The layering is well observed in the central parts of the outcropping area while the intensive subsolidus mylonitic fabrics are well developed at the margins. The mineral lineations are poorly developed. The foliations in the host rocks around PGP are remarkably deflected at the margins of the pluton commonly becoming margin parallel. A dextral shear zone trending NE–SW to N–S passes through the eastern margin of the PGP giving rise to the steeply dipping mylonitic gneisses (Nagaraju and Chetty, 2005).

2.3. Field fabrics

The overall pattern of magmatic foliations show either onionskin/helicoidal signature or the presence of overturned flow folds (with NE-trending axial plane) within the pluton (Fig. 2A). In general, dips vary from steep to moderate values at the margins while they are moderate to gentle in the central parts. However, some local variations in dips are also seen which might be due to local eddy currents. The anorthosite and leucogabbro lenses in the northern part show conformable structural trends with that of gabbro. The foliations are mostly margin parallel, and the axial planes of several isoclinal folds at the eastern margin also trend parallel to the margin. Similar helicoidal/spiral geometry of the foliations can also be observed in the southern part of the pluton, with a crescent shaped anorthosite body in the core. The foliation planes in both the northern and the southern parts of the pluton depict small circle maxima in the stereoplots indicating the conical geometry closing downwards marked by near vertical axes (Fig. 2B and C).

Mineral lineations, though rare, are defined by preferentially aligned plagioclase grains wherever observed. Lineations are oriented in different directions with variable plunges. In general, moderate to steep plunges in the central parts and moderate to gentle plunges at the margins are common. Several mesoscopic folds occur in the northern part plunging either southwest or northeast (40°–60°) and mimic the large-scale overturned folds within the pluton on the map scale. Numerous mesoscopic shear zones characterize the entire eastern margin. At the northern and SE margins, discrete outcrops constitute a structural aureole defined by the deflection of NW-trending gneissic foliations of the country rocks, which gradually become parallel to the margin of the pluton.

2.4. Petrography

The gabbros essentially consist of plagioclase, augite, olivine and orthopyroxene in order of abundance, while biotite, sphene and opaques form accessories. These coarse grained gabbros show hypidiomorphic, cumulate and subophitic textures. Plagioclase grains are subhedral and display albite and Carlsbad–albite twinning, which are deformed at places. Petrographic characteristics suggest that the magmatic fabrics in the pluton are acquired during crystallization when the gabbro is still above the solidus (Nagaraju and Chetty, 2005). The magmatic fabrics are defined by well preserved textures such as coarse grained nature, subheral to euhedral Fe–Mg minerals, triple points between cumulates indicating equilibrium conditions, alignment of plagioclase twins, and alternate enriched portions of mafic and plagioclase grains. Several medium- to high-temperature solid-state deformation microstructures include: reduction in grain size of main mineral phases, intense alignment of mafic and felsic phases and deformational features (erased, bent, kinked twins) in plagioclase grains.

3. AMS studies

3.1. Significance of AMS fabrics

Mineral lineations are crucial in understanding flow mechanism and emplacement history of plutons. The scarcity of mineral lineations in the field makes AMS studies more significant in the present study. The layering of silicate minerals, defined by the tabular cumulus plagioclase, olivine and pyroxene forming a tri-orthogonal fabric, controls the arrangement of magnetite. Thus, magnetite crystallizes always with biotite in the space left by cumulates in late crystallizing fluid rich melt pockets (Ferre, 2002). The interstitial habit of ilmenite and magnetite does not mean that these oxides are crystallized from a late liquid. These oxides represent the liquidus minerals, which might have started crystallizing even before the crystallization of regular cumulates. They can also be formed simultaneously together with silicates and get accumulated with them in the interstitial spaces between the larger silicate crystals. Thus, the opaque sub fabrics mimic the primary petrofabric, which is mainly defined by the common SPO of plagioclase and pyroxene crystals.

3.2. Sample collection and AMS measurements

A total of 107 oriented rock samples, covering the entire range of lithologies of the pluton and the country rocks from well-exposed outcrops, have been collected (Fig. 1B). Sampling sites were precisely positioned with a GPS and were carefully chosen to be away from fractures and weathered portions. Sampling at regular intervals was not possible owing to its irregular and scarce distribution of outcrops. A total of 396 standard cylindrical cores (2.5 cm in diameter and 2.2 cm long) were obtained by making 3–6 cores at each site. The attitudes of layering and/or foliation in the field at these sites were also recorded.

Low field bulk susceptibility (K_m) and other AMS measurements (P', K_1, K_2, and K_3) were carried out with a

KLY-2 Kappabridge (Geofyzica Brno, Czech Republic) at the palaeomagnetic laboratory of Indian Institute of Geomagnetism (IIGM), Alibagh, India. An alternating low field (3.8×10^{-4} T; 920 Hz) AMS was determined with a sensitivity of 2×10^{-7} SI. A sequence of 15 susceptibility measurements along different orientations of the samples was carried out to determine orientation and magnitude of the susceptibility ellipsoid with principal axes $K_1 \geq K_2 \geq K_3$. From this basic data, the mean susceptibility (K_m), strength of magnetic lineation (L) and foliation (F), shape parameter (T), the degree of anisotropy of the susceptibility ellipsoid (P), and its corrected measure (P') were determined (Jelinek, 1981; Tarling and Hrouda, 1993). The calculations of these parameters were carried out using KLY-3 software. Isothermal Remanent Magnetization (IRM) were also measured by a spinner magnetometer (Molspin Ltd, New castle Tyne, UK) and pulsed field magnetizer (maximum field is 1 T).

The paramagnetic minerals like pyroxene, biotite and amphiboles, in general, control AMS dominantly and the long axis K_1 (magnetic lineation) lies parallel to the zone axis of biotites (preferred direction of growth)/mean elongation of mafic minerals. The K_3 defines the short axis that is normal to magnetic foliation, and accounts for the mean preferred planar orientation of Fe–Mg minerals. However, in ferromagnetic rocks like gabbro-norites with high values of K_m, the AMS is related to the shape and distribution anisotropy of magnetite/hematite, which is generally dependent on the rock fabric (Diot et al., 2003).

3.3. Magnetic mineralogy and the source of AMS

The magnetic fabric is primarily related to the petrofabric of the significantly susceptible mineral species. The para- and diamagnetic fabrics would play an important role where magnetite is present in very small amounts in a rock (<0.1 wt%). The nature of AMS can be assumed to be entirely ferromagnetic, if the K_m values are $>10^{-2}$ SI units (Archanjo et al., 1999) and paramagnetic susceptibility values are not likely to exceed 10^{-3} SI units (Rochette, 1987). Various mixtures of ferromagnetic and paramagnetic are known to be the magnetic carriers for K_m values in the range 10^{-4} to 10^{-2} SI units (Ferre, 2002). Anisotropy of susceptibility for dia- and paramagnetic minerals is controlled by crystallographic orientations of mineral grains and is not appreciably influenced by grain shape. For ferromagnetic minerals (like magnetite), AMS is largely controlled by shape anisotropy and distribution (Borradaile and Henry, 1997). Complexities can arise from the post-crystallization magnetite as it has got no relationship with the emplacement fabrics. If the pre-existing magnetites have been strung together to form elongate domains by tectonic deformation, the AMS fabric will not represent the initial fabric. In view of these considerations, it is essential to carefully study the nature of ferromagnetic grains and their relationship with the paramagnetic minerals, as the latter define the magmatic fabrics in layered intrusions. Though equidimensional, magnetite grains are located preferentially along parallel planes or lines, which may raise the susceptibility anisotropy (Hargraves et al., 1991). This explains the nature of well-defined AMS of magnetite in which one cannot detect the shape alignment of magnetite.

Under the microscope, the magnetite grains in the gabbros of PGP occur as part of cumulate textures and are associated with biotites and pyroxenes (Fig. 3A). They range in size from small (<100 μm) to medium grained (~0.5 mm) and are xenomorphic. They mostly occur around the pyroxenes and biotites as intercumulus phase with no apparent shape fabric. These textures suggest that magnetite is mainly a primary mineral. Often, it also occurs as a secondary product in the form of symplectite between pyroxene and magnetite (Fig. 3B) along the faces of pyroxene and as opacitization of biotites. Presence of more domains of magnetite along the faces of pyroxene, association of biotite-magnetites within the layers of pyroxene and the inclusions of magnetite along the cleavage planes of mica indicate their influence in the determination of AMS directional fabrics. The long faces of pyroxenes contain more domains of magnetite and the distribution of anisotropy is crucial in AMS studies. Since most of the biotite–magnetites are attached to the pyroxene layers (Fig. 3C); a planar magnetic fabric is well displayed. The inclusions of magnetite along the cleavage planes of micas are also common in gabbros of PGP, which also might have influenced the AMS directional fabrics. At places, magnetites show intergrowth textures with exsolved lamellae of ilmenite. The distributions of remanance carrying inclusions like ilmenite/magnetite in two perpendicular sets of cleavages that are oblique to the long axis of pyroxene grains also generate orientation fabrics. Considering the abundance of para- and ferromagnetic minerals, the role of the diamagnetic minerals (plagioclase) in AMS studies would be insignificant.

3.4. The mean magnetic susceptibility (K_m)

The Pasupugallu Gabbro Pluton can be described as ferromagnetic as all the plutonic units display high K_m values (4.63×10^{-4} to 5.68×10^{-2} SI; Table 1). Since the K_m is a linear function of iron content in the rock, it can be correlated with the petrographic type of Gleizes et al. (1993). The deformed/mylonitic gabbros provide similar K_m values as that of undeformed gabbros. Leucogabbro-norites possess slightly higher values, possibly due to the presence of orthopyroxene with extensive ilmenite-magnetite schillar exsolved phases. Leptynites show weaker values (in the order of 2.89×10^{-5} SI) due to the dominant paramagnetic contribution while mafic granulites display much higher values (2.07×10^{-3} to 156×10^{-3} SI) because of the presence of ferromagnetic minerals. Most mafic silicates have K_m value higher than that predicted from their chemical composition due to iron oxide inclusions, which will also help in increasing the anisotropy (Hrouda, 2002). The map of K_m iso-value contours shows several concentric and circular lobes within the pluton (Fig. 4A). Higher values can be seen particularly at the eastern, SE, SW and northern sheared margins. The circular feature is related to the central leucogabbro-norite while low values correspond well with anorthosite lenses. The broad progressive increase of K_m values from east to west possibly indicates lateral magmatic flow/differentiation towards west within the pluton. Some gabbros and mylonitic gabbros have yielded lower values which could be due to higher degree of

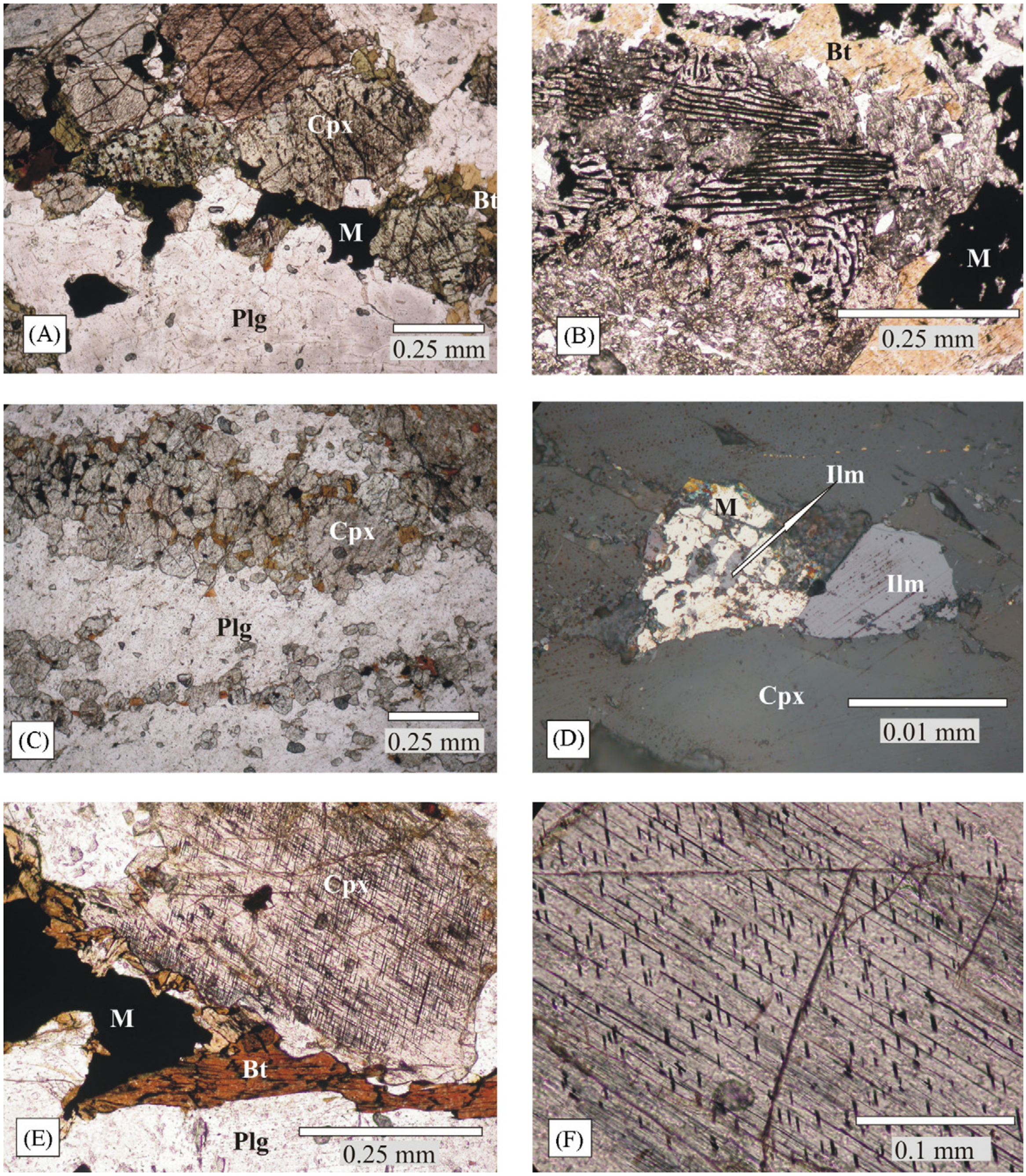

Fig. 3. Photomicrographs of gabbro-anorthosites showing the nature of occurrence and distribution of ferro- and paramagnetic minerals. (A) Association of Primary magnetites with biotite and clinopyroxenes in the cumulus textures, (B) symplectite of magnetite and clinopyroxene, possibly due to the olivine destabilization, (C) distribution of equigranular magnetites in pyroxene layers, (D) ilmenite (grey) and magnetite with ilmenite lamellae grains within the host pyroxene (reflected light), (E) magnetite along the cleavages of biotite and a large magnetite grain (magnetically multidomain), (F) ilmenite lamellae along two sets of cleavages in clinopyroxene as exsolvus phase. Abbreviations used: Clinopyroxenes (Cpx), Plagioclase (Plg), Magnetite (M), Ilmenite (Ilm), Biotite (Bt).

alteration and weathering. However, the bulk K_m histogram (Fig. 5) shows that more than 80% of the data are ferromagnetic ($K_m > 10^{-3}$ SI) and 15% of the data belong to the mixed origin (0.5×10^{-3} SI $< K_m < 10^{-3}$ SI, Borradaile, 2001). In the mixed domain, the K_m is derived from the contributions of both paramagnetic and ferromagnetic fractions.

The frequency distribution histogram of K_m of different litho-units correlates well with the uni-/bi-modal nature of data suggesting the compositional source of susceptibility (Fig. 5B). With the exception of mafic granulites, all other rock types display unimodal frequency distribution of K_m, while secondary product of mafic granulites show bimodal peak. Unimodal frequency distributions of susceptibility within the pluton suggest the influence of single mineral as the dominant source of susceptibility. Bimodal peaks suggest that the source of magnetic susceptibility could be from atleast two strongly susceptible mineral fractions or a combination of two para- and one ferromagnetic mineral.

Table 1
AMS Data for the samples of Pasupugallu Gabbro Pluton

Site	Mean AMS Data			K_1 D/I	K_3 D/I	L	F	P′	T
	N	Rock Type	Km (X 10-3 SI)						
PG 24	4	Gabbro	15.350	158/18	275/30	1.053	1.045	1.1	−0.074
PG 31	4	Gabbro	12.970	326/3	232/37	1.024	1.082	1.113	0.535
PG 41	5	Gabbro	4.640	42/42	262/22	1.03	1.13	1.175	0.611
PG 77	6	Gabbro	7.910	267/36	2/5 3	1.041	1.135	1.191	0.514
PG 78	6	Gabbro	4.270	274/81	133/5	1.079	1.019	1.106	−0.595
PG 85	5	Gabbro	0.794	267/5	358/76	1.026	1.108	1.145	0.597
PG 86	6	Gabbro	5.450	218/46	73/18	1.048	1.054	1.104	0.055
PG 87	3	Gabbro	46.250	148/58	323/2	1.008	1.021	1.03	0.427
PG 90	5	Gabbro	21.400	270/12	4/6 8	1.026	1.076	1.107	0.473
PG 91	4	Gabbro	30.620	162/62	308/14	1.005	1.038	1.047	0.782
PG 92	6	Gabbro	2.130	199/8	291/78	1.08	1.222	1.331	0.444
PG 101	5	Gabbro	56.530	133/37	334/11	1.01	1.073	1.091	0.757
PG 102	6	Gabbro	2.290	158/78	291/8	1.041	1.009	1.053	−0.649
PG 118	5	Gabbro	0.463	220/16	88//17	1.008	1.02	1.029	0.429
PG 119	3	Gabbro	1.330	204/10	105/45	1.076	1.075	1.156	−0.006
PG 139	5	Gabbro	39.940	248/35	6/3 7	1.033	1.029	1.063	−0.059
PG 142	6	Gabbro	1.530	140/67	319/0	1.036	1.13	1.18	0.548
PG 143	4	Gabbro	1.450	66/9	166/39	1.048	1.007	1.061	−0.759
PG 144	6	Gabbro	4.310	327/24	194/22	1.047	1.083	1.135	0.27
PG 145	5	Gabbro	3.240	315/25	189/27	1.051	1.03	1.084	−0.256
PG 146	4	Gabbro	5.040	311/57	192/27	1.055	1.028	1.087	−0.318
PG 147	6	Gabbro	3.540	302/20	161/14	1.015	1.049	1.068	0.53
PG 160	3	Gabbro	16.210	343/34	189/13	1.066	1.159	1.243	0.397
PG 164	3	Gabbro	5.270	93/37	308/18	1.027	1.056	1.086	0.34
PG 167	3	Gabbro	15.240	195/51	47/16	1.026	1.026	1.053	0.012
PG 169	3	Gabbro	15.330	268/7	44/7	1.047	1.047	1.097	0.005
PG 170	3	Gabbro	16.460	324/18	163/57	1.009	1.096	1.118	0.81
PG 171	3	Gabbro	12.940	360/16	184/10	1.039	1.071	1.115	0.272
PG 174	3	Gabbro	10.070	25/85	181/2	1.036	1.065	1.105	0.287
PG 175	3	Gabbro	10.930	51/13	148/58	1.001	1.055	1.064	1.097
PG 176	3	Gabbro	18.280	40/8	308/75	1.007	1.03	1.04	0.606
PG 177	3	Gabbro	11.620	124/85	234/4	1.082	1.07	1.158	−0.073
PG 178	3	Gabbro	19.350	328/15	63/67	1.051	1.015	1.071	−0.53
PG 179	3	Gabbro	7.100	286/52	48/28	1.043	1.055	1.101	0.122
PG 200	3	Gabbro	39.540	50/12	296/25	1.046	1.103	1.157	0.373
PG 216	3	Gabbro	56.840	1 0/3	279/68	1.037	1.021	1.06	−0.283
PG 219	4	Gabbro	4.460	337/67	155/1	1.059	1.067	1.131	0.062
PG 220	3	Gabbro	27.650	205/61	54/13	1.023	1.02	1.043	−0.067
PG 223	3	Gabbro	20.360	358/16	252/42	1.104	1.088	1.201	−0.08
JN 223	2	Gabbro	31.720	206/26	355/14	1.03	1.203	1.263	0.723
PG 227	3	Gabbro	21.740	220/7	124/51	1.004	1.261	1.309	0.967
PG 229	3	Gabbro	12.370	23/46	176/14	1.044	1.022	1.069	−0.331
PG 235	3	Gabbro	44.390	72/34	277/12	1.053	1.072	1.129	0.146
PG 236	3	Gabbro	51.750	65/40	283/20	1.046	1.069	1.119	0.19
PG 237	3	Gabbro	39.760	237/22	275/67	1.076	1.294	1.415	0.559
PG 242	3	Gabbro	11.320	249/20	342/68	1.216	1.39	1.701	0.254
PG 11	4	LeucoGabbro	5.670	23/44	289/46	1.014	1.004	1.019	−0.524
PG 39	6	LeucoGabbro	4.270	61/21	262/7	1.042	0.028	1.072	−0.195
PG 43	6	LeucoGabbro	70.680	344/35	120/23	1.042	1.03	1.074	−0.161
PG 96	5	LeucoGabbro	1.710	10/3 7	258/42	1.06	1.148	1.223	0.407
PG 98	5	LeucoGabbro	1.590	314/77	139/1	1.038	1.017	1.056	−0.386
PG 114	3	LeucoGabbro	11.760	22/11	340/8	1.02	1.131	1.168	0.726
PG 115	3	LeucoGabbro	11.680	116/21	339/17	1.012	1.157	1.192	0.848
PG 117	6	LeucoGabbro	1.230	117/62	242/22	1.052	1.082	1.139	0.221
PG 136	6	Leucogabbro	25.030	185/1	276/60	1.007	1.13	1.156	0.894
PG 202	3	Leucogabbro	20.520	50/44	164/38	1.071	1.048	1.123	−0.195
PG 203	3	Leucogabbro	19.150	220/63	48/2.5	1.024	1.338	1.422	0.853
PG 205	1	Leucogabbro	11.630	236/29	72/7	1.047	1.108	1.163	0.383
PG 209	3	Leucogabbro	8.180	246/73	44/6	1.061	1.145	1.221	0.389
PG 211	3	Leucogabbro	6.340	348/63	220/20	1.043	1.143	1.202	0.518
PG 221	3	Cumulates	21.870	348/27	243/49	1.039	1.21	1.278	0.665
PG 18	4	Anorthosite	15.680	200/33	327/28	1.057	1.063	1.123	0.045

Table 1 (*Continued*)

Site	Mean AMS Data			K_1 D/I	K_3 D/I	L	F	P′	T
	N	Rock Type	Km (X 10-3 SI)						
PG 134	5	Anorthosite	10.610	280/82	154/6	1.026	1.078	1.111	0.497
PG 163	3	Anorthosite	10.700	341/14	248/73	1.038	1.125	1.176	0.519
PG 180	3	Anorthosite	12.950	360/14	266/71	1.085	1.096	1.189	0.06
PG 181	3	Anorthosite	29.420	232/13	323/77	1.027	1.111	1.15	0.597
PG 182	3	Anorthosite	21.220	165/35	02/0 8	1.048	1.018	1.069	−0.445
PG 206	3	Anorthosite	20.470	42/41	244/11	1.043	1.249	1.329	0.68
PG 207	3	Anorthosite	8.980	69/41	238/6	1.021	1.217	1.27	0.808
PG 210	3	Anorthosite	11.080	112/50	347/28	1.033	1.129	1.176	0.581
PG 93	4	Dolerite	0.504	36/20	230/5	1.004	1.016	1.021	0.592
PG 94	5	Dolerite	0.472	249/14	36/9	1.012	1.057	1.075	0.644
PG 95	5	Dolerite	71.080	263/34	130/25	1.081	1.023	1.111	−0.555
PG 184	3	Dolerite	71.560	192/14	59/80	1.008	1.048	1.061	0.684
PG 104	3	Mylonitie gabbro	2.400	209/6	118/80	1.123	1.315	1.492	0.404
PG 106	3	Mylonitie gabbro	0.571	126/34	280/13	1.021	1.074	1.101	0.542
PG 107	6	Mylonitie gabbro	11.330	41/59	180/18	1.034	1.209	1.272	0.697
PG 108	4	Mylonitie gabbro	0.886	144/29	44/56	1.004	1.018	1.024	0.613
PG 109	6	Mylonitie gabbro	59.210	96/66	238/14	1.118	1.113	1.245	−0.02
PG 111	3	Mylonitie gabbro	0.041	277/48	74/11	1.023	1.067	1.095	0.485
PG 124	4	Mylonitie gabbro	7.580	179/28	354/2	1.022	1.055	1.08	0.426
PG 156	1	Mylonitie gabbro	3.030	156/24	5/1 2	1.02	1.09	1.119	0.623
PG 214	3	Mylonitie gabbro	0.641	317/28	63/50	1.011	1.026	1.038	0.401
PG 122	6	Mafic granulite	4.670	172/69	300/16	1.045	1.043	1.09	−0.021
PG 126	2	Mafic granulite	155.550	101/5	194/57	1.214	1.1785	1.4315	−0.0835
PG 127	5	Mafic granulite	118.660	225/16	120/43	1.219	1.05	1.299	−0.602
PG 129	5	Mafic granulite	2.280	58/68	169/20	1.065	1.069	1.138	0.033
JN 129	5	Mafic granulite	60.720	43/72	170/14	1.057	1.059	1.12	0.016
PG 130	6	Mafic granulite	129.250	155/73	320/4	1.266	1.064	1.369	−0.585
PG 131	3	Mafic granulite	89.210	109/52	240/25	1.132	1.205	1.367	0.202
PG 189	3	Mafic granulite	61.660	208/57	309/32	1.243	1.101	1.379	−0.388
PG 197	3	Mafic granulite	2.070	197/33	1 1/3	1.085	1.061	1.152	−0.161
PG 198	3	Mafic granulite	3.580	305/61	207/29	1.07	1.121	1.202	0.257
PG 208	3	Mafic granulite	11.360	54/8	307/24	1.086	1.156	1.259	0.278
PG 225	3	Mafic granulite	16.180	67/61	236/5	1.054	1.112	1.175	0.339
PG 226	3	Mafic granulite	28.820	349/1.3	251/84	1.102	1.16	1.281	0.208
PG 228	3	Mafic granulite	8.340	338/51	157/0	1.027	1.102	1.139	0.571
PG 191	3	Amphibolite	14.110	240/13	350/30	1.037	1.274	1.354	0.739
PG 56	3	Mylonitic gneiss	4.100	346/20	162/1	1.013	1.128	1.159	0.812
PG 79	5	Leptynite	10.620	281/49	96/3	1.073	1.111	1.194	0.201
PG 83	5	Leptynite	14.080	194/45	331/23	1.197	1.159	1.387	−0.099
PG 152	3	Leptynite	0.029	293/71	134/6	1.112	1.114	1.239	0.009
PG 218	3	Leptynite	0.288	13/22	108/64	1.029	1.023	1.053	−0.103
PG 230	3	Leptynite	0.390	17/21	258/31	1.088	1.164	1.27	0.288
PG 239	3	Leptynite	5.290	357/45	155/12	1.057	1.06	1.121	0.027
PG 240	3	Leptynite	4.290	75/12	335/46	1.033	1.171	1.226	0.657
PG 241	3	Leptynite	2.390	5/3 6	120/39	1.046	1.129	1.188	0.464

N: number of cores from each site that were used to compute mean values, K_m: mean magnetic susceptibility, K_1 and K_3: long and short axis of the magnetic susceptibility ellipsoid, D: declination, I: inclination, L: magnetic lineation, F: magnetic foliation, P′: corrected degree of anisotropy, T: shape anisotropy.

3.5. Degree of magnetic anisotropy (P′) and shape parameter (T)

The AMS strength and shape have been derived using the P' and T parameters, respectively (Jelinek, 1981):

$$P' = \exp\sqrt{2}\left[\left\{\ln\left(\frac{K_1}{K_m}\right)\right\}^2+\left\{\ln\left(\frac{K_2}{K_m}\right)\right\}^2+\left\{\ln\left(\frac{K_3}{K_m}\right)\right\}^2\right] \quad \text{and}$$

$$T=\left[\frac{\{2(\ln K_2-\ln K_3)\}}{\{\ln K_1-\ln K_3\}}\right]-1$$

The gabbros show a range of P' values from 1.09 to 1.701, while the anorthosite and leucogabbro-norites show relatively lower values (1.0–1.4) (Table 1). The P' contour map (Fig. 4B) shows high degrees of anisotropy at most of the margins ($P' > 1.4$) while the central parts have lower P' values (<1.05). The central parts thus represent a near spherical AMS ellipsoid. The P′ distri-

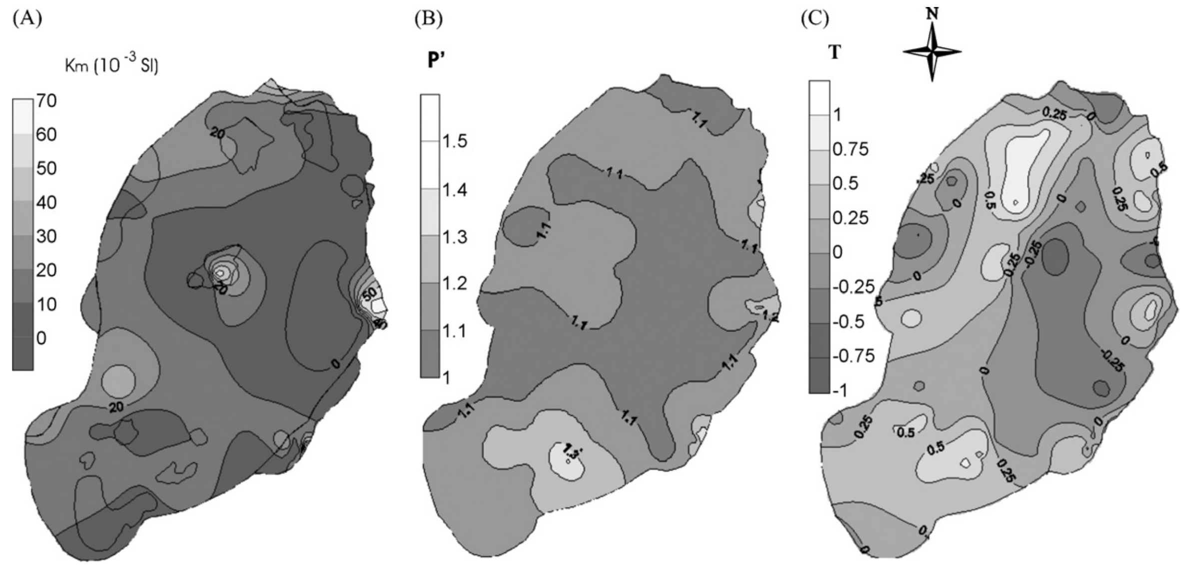

Fig. 4. Contoured maps for (A) Magnetic susceptibility, K_m, (B) degree of anisotropy P′, and (C) shape parameter, T of the Pasupugallu pluton.

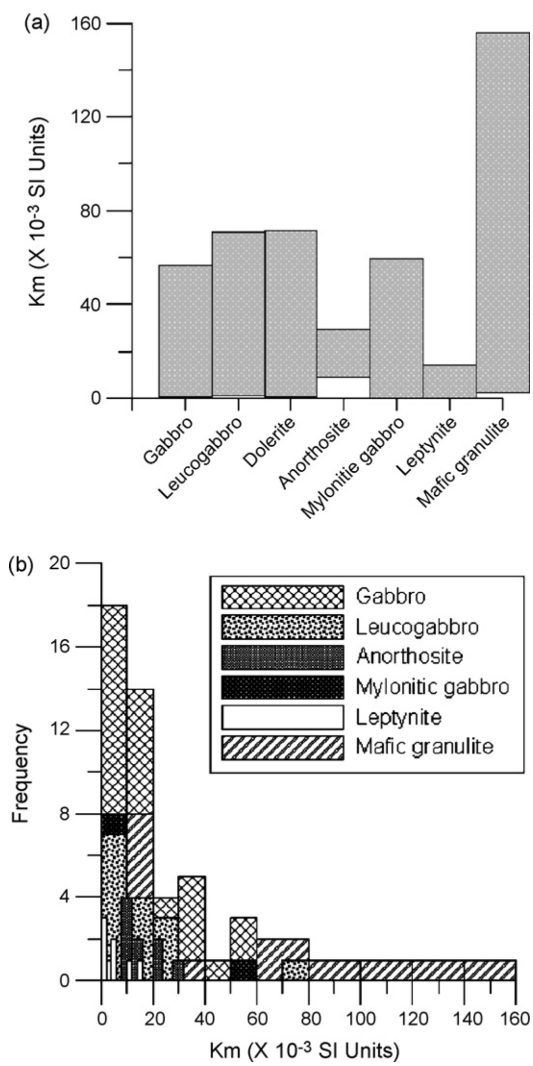

Fig. 5. (A) Histogram showing the ranges of magnetic susceptibility (K_m) of the various lithologies of the pluton along with host rocks. (B) Frequency histogram showing the K_m values for all lithologies.

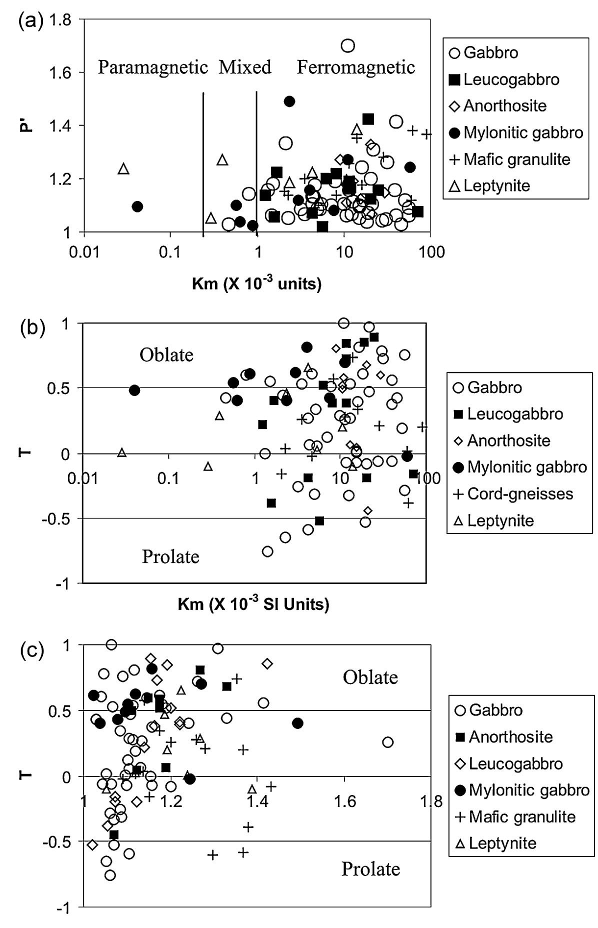

Fig. 6. (A) Graph of Degree of Anisotropy (P′) vs. Magnetic susceptibility (K_m), (B) Shape Parameter (T) vs. Magnetic susceptibility (K_m), and (C) (P′ vs. T) plot after Jelinek (1981).

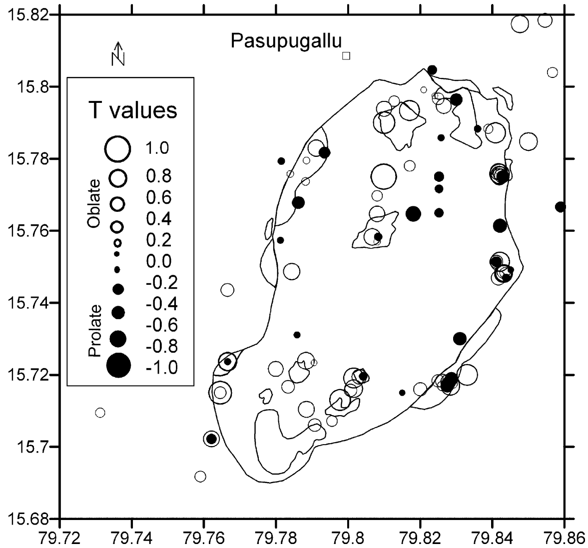

Fig. 7. Map showing the distribution of shape parameter (T) of magnetic susceptibility in and around PGP.

bution shares a similar contour pattern with that of K_m, with the exception of highly susceptible SW-margin of the pluton. The graph P' vs. K_m (Fig. 6A) shows an apparent linear correlation between the two with all the rock types falling in the ferromagnetic domain except a few that belong to mixed domain. Some leptynites and one sample of mylonitic gabbro fall in the domain of paramagnetic field.

The magnetic shape parameter T is used here to characterize the shape of magnetic susceptibility ellipsoid (Jelinek, 1981; Borradaile, 1988). The plutonic units are dominated by positive T values. Gabbros show a wide range of T values (from −0.7 to 0.9) (Table 1), but the mean value corresponds to oblate (+ve) field. In general, the central parts are dominated by oblate ellipsoid while most of the margins show prolate types with the exception of the eastern margin (Fig. 4C). No apparent correlation exists between T vs. K_m (Fig. 6B), but most of the data falls in the oblate domain. Though the correlation between P' vs. T is ambiguous, the gabbros and leucogabbros tend to fall in the oblate field as the anisotropy increases (Fig. 6C). Mafic granulites show both prolate and oblate ellipsoids while leptynites show prolate to near plano-linear fabrics. A few prolate ellipsoids in the central parts gradually change to oblate towards west suggesting that the magma might have spread to the east and west from the central part after the ascent/emplacement (Fig. 7). Thus, it is possible that the T values are variable within the same lithology and can be used as deformational indicator. This is further supported by the presence of prolate ellipsoids at the eastern margin and dominant oblate ellipsoids at the western margin. From these observations, we interpret that the strain at the contact between the host and pluton could be constrictional (dip-slip) near the eastern margin while flattening strain is dominant at the western margin. The southern domain and some parts near the northern margin show strong planar fabrics ($T > 0.25$). The AMS planar fabrics observed in the pluton reflect distinctly on the nature of magnetic mineralogy of rocks and the fabrics could represent primary feature acquired during the emplacement of magma. Further, the prolate T values obtained in the present study indicate that the internal dynamic forces have significantly influenced the foliation fabrics of Pasupugallu Pluton when compared to the gravitational forces (Tarling and Hrouda, 1993).

3.6. Magnetic directional data

The measured magnetic fabric orientations are found to be consistent from all core samples within the single site. The absolute mean angular directional variability (α) of K_m and K varies from 0 to 40°. The geometry of magnetic foliations is generally in accordance with the magmatic planar fabrics in the field. Magnetic foliations of the Pasupugallu Pluton trend mostly in all directions with moderate to gentle dips displaying a helicoidal pattern (Fig. 8A). In the northern domain, two major planes trending NE–SW and NW–SE with variable dips can be deduced from stereoplot of poles to foliations (Fig. 8B), which are conformable to the alignment of overturned magmatic folds. In the southern domain, the poles to foliations (Fig. 8C) display an axis trending NNE–SSW (parallel to the long axis of the pluton) with gentle to moderate dips on either side.

3.6.1. Magnetic foliation trajectories

Most of the magnetic foliations are conformable with the margins of the pluton with the exception at the northern margin (Fig. 8A). The magnetic fabrics, commonly mimicking the field fabrics, show a progressive rotation from center to margins. In the central part, foliation is very steep which gradually becomes moderate to gentle at the margins. However, the eastern margin is characterized by steep dips. In the southern domain, steep foliations in the central part and moderately dipping foliations at the margins give rise to onion-skin like pattern. In general, the foliations throughout the pluton are dominantly inward dipping. But, outward dips are also common at the northern and southeastern margins, which are consistent with the field fabrics. The magnetic foliation trajectories show alternative domains of gentle/moderate/steeply dipping layers in both northern and southern parts (Fig. 8A–C). There seems to be broad correlation between magmatic and magnetic foliations. Two prominent NE–SW trending shear zones (dark gray shaded portions) can be delineated in both northern and southern parts of the pluton and the magnetic foliations are deflected in a dextral pattern giving rise to overturned fold pattern. The SW- and eastern margins are characterized by gentle dips while the northern margin is characterized by steep inward dips. Steep dips are striking in the central parts with moderately plunging lineations. The measured magmatic foliations in the host rocks (Fig. 8D) show predominant NE–SW trends with steep dips on either side. A few NW–SE trending foliation are also common.

3.6.2. Magnetic lineations

The magnetic lineations are, in general, concentrically distributed with steep to gentle plunges, which are widely spread in stereoplots (Fig. 9B and C). Although, the lineations in the field are limited with in the pluton, there is close correlation between the observed lineations in the field and magnetic lineations that

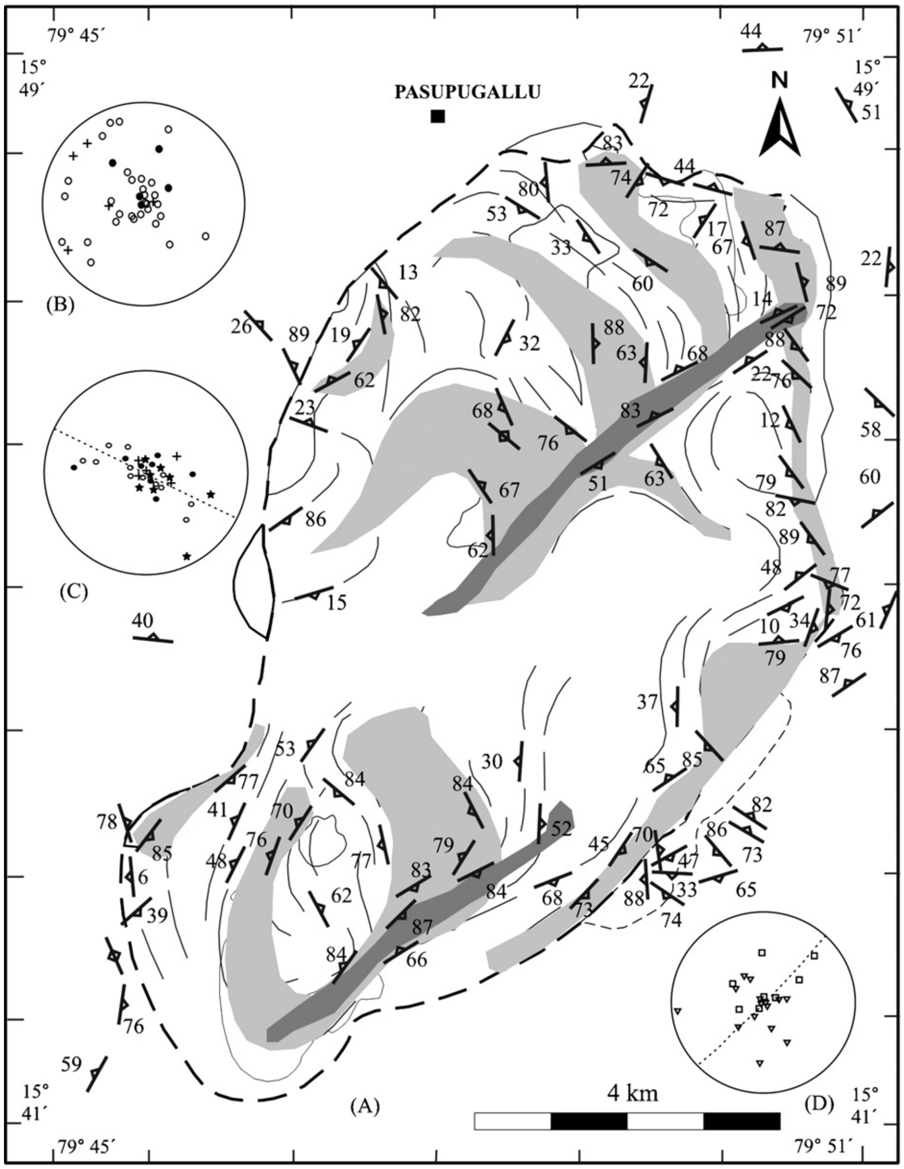

Fig. 8. (A) Magnetic foliation trajectory map of PGP. Lower hemisphere equal area projection of poles to the magnetic foliations in the northern half (B), southern half (C), and host rocks (D). The steeply dipping regions are shown by light shaded portions and the dark gray shaded portion reflects the zone of deflection of foliations delineating Riedel shear zones. (symbols used in stereoplots; ◯ = gabbro; ● = leucogabbro; ⋆ = mylonitic gabbro; + = anorthosite; □ = leptynite; ▽ = mafic granulite).

were measured from AMS studies. Majority of magnetic lineations are margin parallel while outward radial flow patterns are common along the eastern margin (Fig. 9A). Lineation trajectories distinctly show a circular flow pattern representing northern and southern lobes of the pluton. The lineation flow lines also define another broad circular lobe at the eastern margin. However, in the southern lobe, margins are characterised by gentle plunges while the central parts are by steep to moderate plunges (Fig. 9C). This clearly indicates that the magma ascent was in the central parts with a lateral spread or by inclined flow towards the margins, which is consistent with the concept of helicoidal flow (Hippertt, 1994). It is evident from the geometry of lineation trajectories that the magma has flown outward spirally from the central parts towards the margins.

Significant variations in plunge directions can be noticed in the central parts as well as at the margins. These can be attributed to the sudden changes in the layer flow from prolate to oblate strain pattern either during the helicoidal flow or during flow folding. The plunges vary from steep to sub-horizontal with majority of them showing gentle to moderate values even within a single circular lobe (Fig. 9A). The apparent three circular lobes that are delineated in the pluton may suggest three possible centers of magmatic pulses. The magnetic lineation trajectories also display two prominent NE–SW trending shear zones (dark gray portions) similar to those displayed by magnetic foliation trajectories. The radial pattern of lineations near NE-margin might indicate local upward convection within the magmatic chamber or the interaction of magma with the host rocks during the flow.

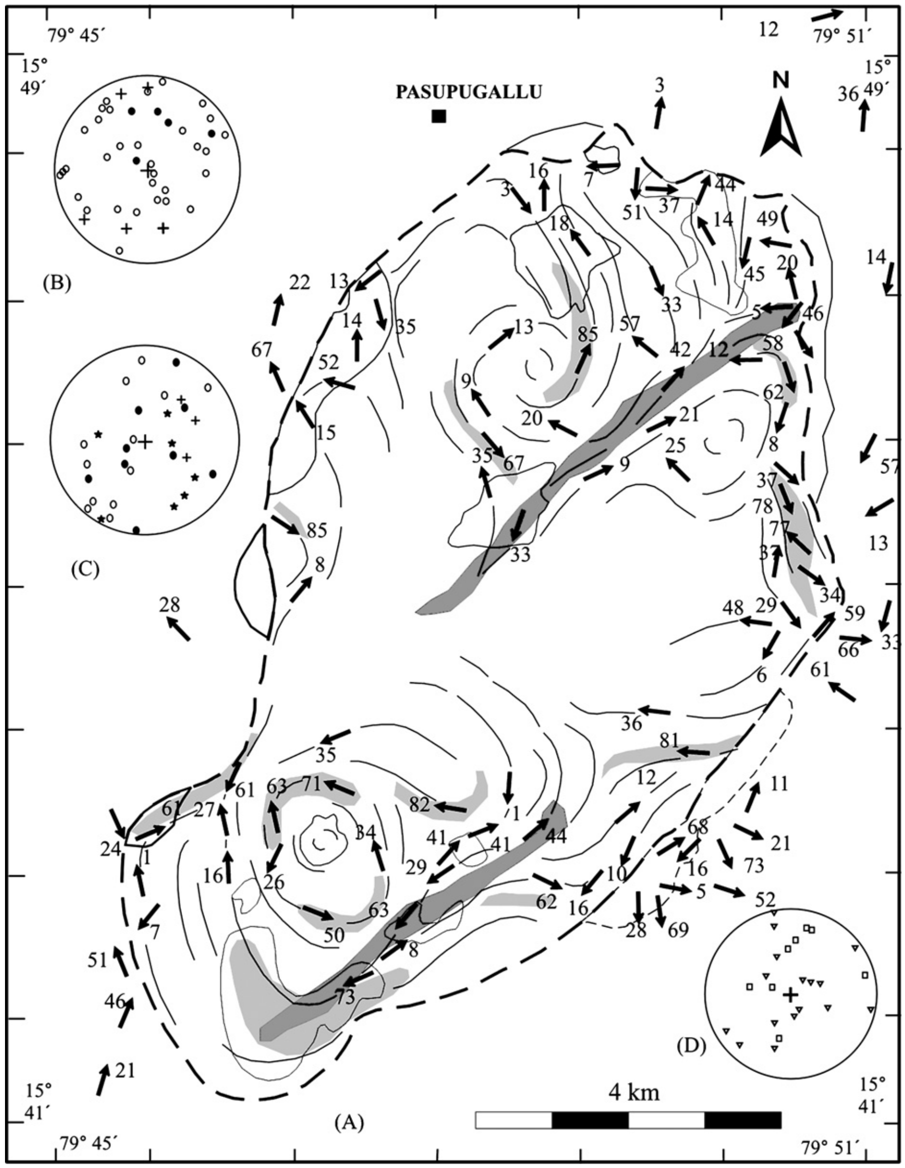

Fig. 9. (A) Map of magnetic lineations and their trajectories in PGP. Lower hemisphere equal area stereoplots for magnetic lineations in the northern half (B), southern half (C) of PGP and in host rocks (D). The steeply dipping regions are shown by light shaded portions and the dark gray shaded portion reflects the zone of deflection of foliations. (symbols used in stereoplots; ◯ = gabbro; ● = leucogabbro; ⋆ = mylonitic gabbro; + = anorthosite; □ = leptynite; ▽ = mafic granulite).

All the magnetic lineations plunge in different directions but predominantly either north or south in the host rocks at the western contact of the pluton (Fig. 9D). East of the pluton, the lineations plunge towards south or SE. These linear fabrics and the deflection of foliations in the wall rocks on either side of the pluton are consistent with regional dextral shear kinematics. Alternatively, the pattern of magnetic lineations also implies that either anti-clock wise up motion of magma or the clock-wise plani-spiral flow of magma with the possible top surface of inward dipping and downward closing crystal mush.

4. Isothermal Remanent Magnetization (IRM) studies

In order to detect the dominant magnetic carrier contributing to the AMS, IRM curves have been constructed for some representative cores at room temperature after subjecting them to an external field (H), which is ramped from 0 to 1 T, and 0 to −500 mT. All the gabbros are saturated before or near 200 mT except the sample PG-143, which is saturated near 300 mT (Fig. 10). Anorthosites, leucogabbros and host mafic granulites have been saturated near 150 mT. These rock types have reached full magnetization at low applied voltages, which is a characteristic behaviour of magnetite (Dunlop, 1986). Leptynites show slightly higher values of saturation, i.e. from 400 to 500 mT, which implies the mixed origin as well as the presence of hematite. IRM results are consistent with high K_m values, demonstrating the control of magnetite on rock magnetic properties. The normalized IRM spectrum displays similar trends and the pattern, which suggest large grain size. The comparison of these curves with the empiri-

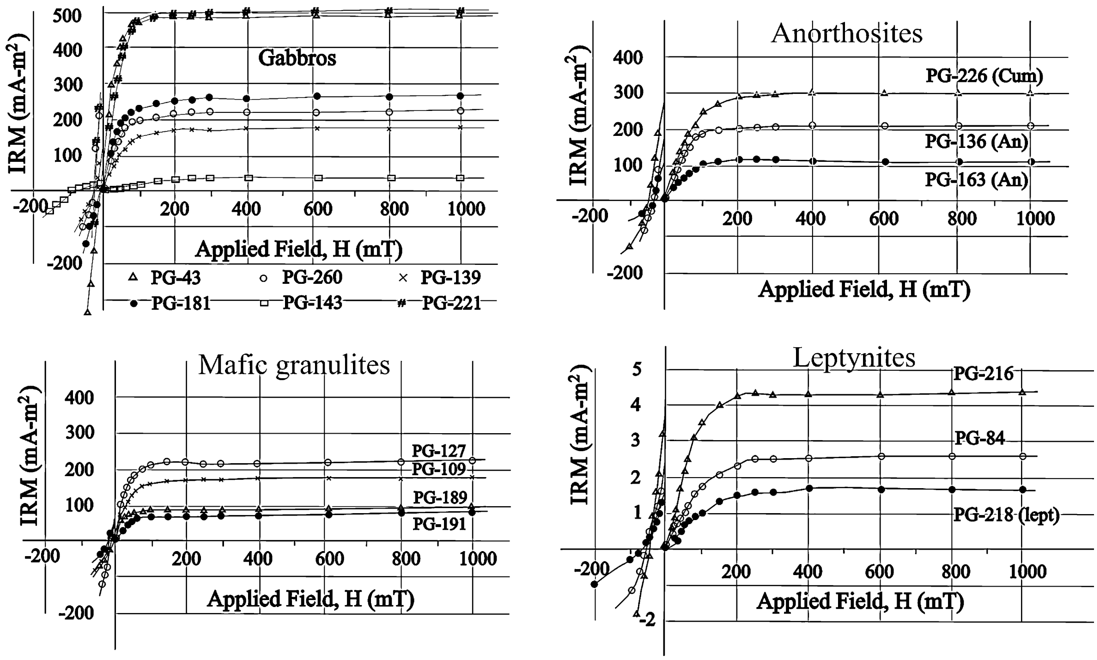

Fig. 10. Hysteresis curves determined for gabbros and anorthosites of the PGP and for the host rocks (mafic granulites and leptynite) from the Induced Remanent Magnetic (IRM) studies.

cal curves of Dunlop (1986) reveals that the magnetic carrier is multi-domain to pseudo-single domain magnetite (Fig. 11). Petrographic studies have also revealed the large grain sizes of magnetite, which are in tune with IRM studies. These grains range in size from 10 μm to more than 100 μm and belong to multi-domain magnetite class (Day et al., 1976; Dunlop, 1986).

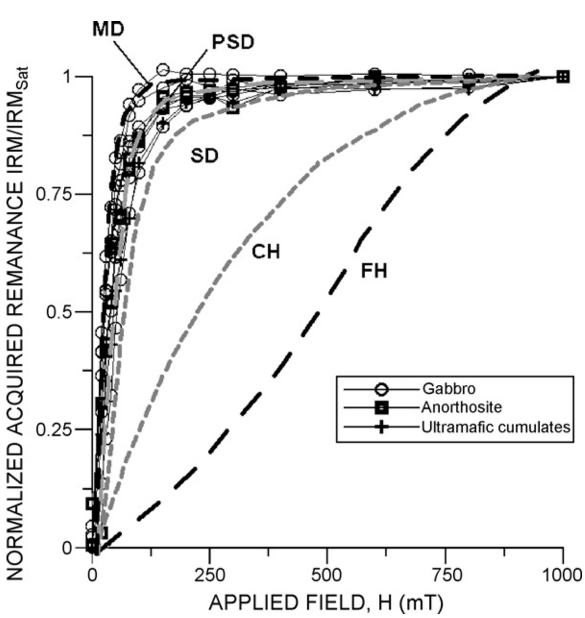

Fig. 11. Normalized hysteresis spectra of the specimens and their comparison with the Dunlop (1986) curves. Magnetite can behave as MD-Multi-Domain, PSD-Pseudo-Single Domain, SD-Single Domain and Hematite as CH- Coarse Hematite and FH- Fine Hematite.

5. Discussion

5.1. Correlation of AMS fabrics and the field observations

The K_m values show good variation from leucogabbros and anorthosite layers to gabbros reflecting lithological changes within Pasupugallu Gabbro Pluton. However, the similar range of K_m values for both gabbros and leucogabbros and the similarities in magnetic fabrics among all plutonic lithounits support the hypothesis that the magnetic carriers of these rocks might be identical and must have been subjected to identical stress fields or dynamic conditions during the emplacement. The relatively higher degree of P' towards the sheared margins indicates a close correlation between the increase of AMS values and the intensity of magmatic deformation. The field fabrics and the rock texture exhibiting weak to strong foliation from centre to the margins also support such a correlation. The magnetic foliations and their trajectories broadly show an excellent correlation with the magmatic foliation in the field. This suggests that the magnetic lineations measured from AMS studies can be considered as the indicators of the magma flow patterns despite the scarcity of mineral lineations in the field.

5.2. AMS fabrics and geometry of PGP

The eastern margin and some parts of the western and northern margins show steeply dipping magnetic foliations indicating that the pluton has inwardly dipping steep walls. In the southern domain, the central lobe is dominated by steep to sub vertical dips conformable with steep lineations, while the layers between the margin and central parts exhibit moderate dips. The magnetic lineation trajectories also define circular/spiral pattern in the form of lobes in both northern and southern domains. Lineations are mostly margin parallel, but radial distribution of moderately to sub horizontally plunging lineations at northern and eastern margins imply a lateral flow of magma towards the margins from the central part in the northern domain. In the southern domain, while the margins are marked by moderate to gentle plunges, the central lobes are characterized by steep plunges indicating that the ascent of magma was in the central parts. The upward migration and lateral spread of magma must have been generated from the same stress pattern. The changes in the behavior of lineations, at some places, could be due to strain variation during the magmatic flow in the form of helicoidal/spiral pattern, which could be related to transpressional deformation along the boundary shear zones.

The NE–SW trending dextral shear zones inferred from the deflection of magnetic foliation and lineations separating two cells/circular lobes in the pluton may suggest the presence of sympathetic and coeval Riedel shear zones developed during the regional dextral transpressional shear kinematics. Further, the same is not reflected in the P' contour diagram, perhaps ruling out the possibility of post emplacement shearing. These observations and the helicoidal fabrics of the pluton can strongly be ascribed to syn-kinematic regional shearing (Patterson and Fowler, 1993).

5.3. AMS fabrics and deformation

The petrographic studies reveal that the marginal gabbros throughout the pluton are mylonitized and display solid-state deformational fabrics. However, the K_m values of these rocks are very much in similar range to those of undeformed gabbros from the central parts. It implies that the deformation has not significantly influenced magnetic fabric of the gabbros even at the margins of the pluton. This can be ascribed to the cooling history of the pluton during the emplacement. We suggest that the pluton must have cooled from its near-emplacement to further lower temperatures while expanding laterally and the interaction between the marginally cooled gabbros and cold country rocks might have given rise to such mylonitic fabrics. Therefore, the observed solid-state fabrics are likely to be coeval with the late stages of emplacement, but not related to the post-emplacement deformational event.

Further, relatively low P' values obtained throughout the pluton (1.1–1.3) when compared to those at the highly strained margins (1.4–1.6) preclude the post- emplacement deformation of plutonic body. All these observations suggest that synchronously developed fabrics within the pluton and the possible manifestation of folding in the form of a plani-spiral flow can be ascribed to syn-emplacement mechanism during the external deformational events in the region.

5.4. Magnetic strain variations, emplacement models and regional tectonics

The progressive increase of K_m from east to west can be considered as the lateral differentiation of the pluton or the tilting of the magmatic chamber at a later time by the westward thrusting/compressional tectonics. The change of prolate to oblate strain ellipsoid from east to west and partly from central parts can also be interpreted as either due to tilting of the eastern part of the magma chamber or due to the steep ascent of the magma in the eastern part with lateral spreading towards the west. The latter possibility suggests shortening of the host rocks, which can be related to westward thrusting. Alternatively, it can also be interpreted that the pluton was emplaced initially as laccolith/lopolith like structure (still during the subsolidus state) with normal sub-horizontal or moderately dipping magmatic layering, which must have been uplifted and tilted towards west or northwest. However, it is pertinent to note that both the models are involved with compressional regime during the emplacement.

The features like helicoidal flow trajectories, transition from magmatic to mylonitic fabrics towards the margins, presence of marginal dextral strike–slip shear zone (Nagaraju and Chetty, 2005), deflection of magnetic foliations and lineations along the Riedel shear zones within the pluton, internal flow folds, shape and long axis of the pluton, remarkable changes in the lineation patterns at the margins, the dominant constrictional magnetic strain ellipsoids, all suggest syntectonic emplacement of the pluton. Based on our mesoscopic as well as regional scale field observations (Nagaraju and Chetty, 2005) and the AMS results obtained from the present study, we infer that the dextral transpressional tectonics between EGMB and EDC might have given rise to local extensional voids or dilatational jogs, into which the magma has been emplaced with possible rotation while the marginal deformation was continuing. This inference is consistent with the experimental deformation studies, which indicate that the directions of magnetic susceptibility spin rapidly with advancing strain, especially where the matrix grains undergo crystal- plastic deformation (Borradaile, 1988). The eastern part seemed to have been affected by regional-scale shearing strain, most probably during the final stage of its emplacement along with magma spreading to the west. This is reflected at the western part in the form of relatively low deformation providing a strain shadow. We also interpret that the magma has risen vertically mainly along the two lobes in north and southern domains in a spiral fashion and extended westwards laterally. The NE–SW linear distribution of elliptical plutons of Prakasam Igneous Province in the transition zone and the presence of marginal shear zones suggest the role of possible transpressional tectonics in controlling the emplacement of ascending magmas that have formed at different levels of lower crust. Our results are also in accordance with the recent magma emplacement models of Cruden (1998), where complex intrusive relationships, pluton infilling by one or more vertical conduits associated with inward dipping structures have been predicted. Similar kind of mechanism for the emplacement of a granitic pluton has also been recently described within a transpressive shear zone from the Borberoma Province, northeast Brazil (Archanjo et al., 1999).

Available geochronological data suggests that early metamorphism in the region (∼1670 Ma, Mezger and Cosca, 1999) is followed by a contemporaneous lithospheric thinning event with emplacement of extensive alkaline magmas during extensional tectonics (∼1450–1300 Ma, Sarkar and Paul, 1998; Sengupta

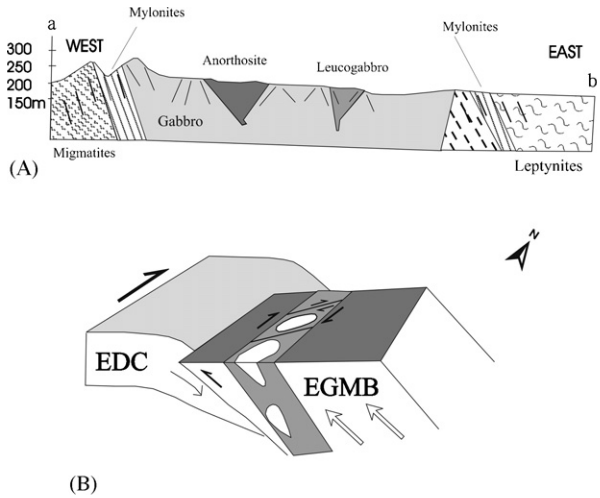

Fig. 12. (A) Schematic E-W cross-section showing the inward dipping, conical shaped (closing downward) Pasupugallu pluton with internal differentiated products with boundary shear zones. (B) Cartoon illustrating the emplacement of mafic magmas along the weak zones (shear zones) provided by the transpressional tectonic setting between the East Dharwar craton (EDC) and the Eastern Ghats Mobile Belt (EGMB).

et al., 2001). More recently, it has been proposed that an initial event of rifting prevailed during the Mesoproterozoic period and the same was converted to collision/subduction during the Neoproterozoic to Pan-African times (Dasgupta and Sengupta, 2003; Upadhyay et al., 2006) thus leading to the development of gneissic foliation within alkaline intrusives. Thus the unmetamorphosed PGP clearly postdate the alkaline gneisses and rules out the possibility of its emplacement during Mesoproterozoic. Considering all these observations as described above, we propose the emplacement of PGP and the presence of transpressional tectonics during the onset of Grenvillian event (1000–900 Ma) in the region. The pre-existing crustal anisotropy probably guided the ascent and final emplacement of the magma (Fig. 12B). It can be summarized that the emplacement of plutonic bodies could be contemporaneous with prolonged transpressional tectonic regime with a dextral strike–slip component along the Transition zone or the Terrane Boundary Shear Zone.

6. Conclusions

The IRM studies combined with petrographic characteristics and the higher K_m values indicate that the gabbroic rocks of the pluton are associated with multi-domain/pseudo-single domain magnetite. Hence, the ferromagnetic contribution is mainly from magnetite, which is also reflected by the presence of normal AMS fabrics and the absence of inversion fabrics (Rochette et al., 1992) within the Pasupugallu Pluton (PGP). The magnetic lineations were proved to be extensively useful in this study, as they provide vital information regarding the magma flow, which was otherwise not possible from the field studies. The AMS data and the field observations suggest that the pluton is a conical body closing downwards (Fig. 12A) with subvertical axis in the northern domain and moderate to steep axis plunging to southwest in the southern domain. The pattern of magnetic directional data suggests that the mafic magma is likely to have ascended from different centers separated by internal shear zones and must have extended towards western parts of the pluton. The helicoidal foliation and lineation trajectories, consistent with the kinematics of marginal shear zones, suggest that the pluton is synkinematic with the regional dextral transpressional tectonics. The shape of the pluton, remarkable changes in the behaviour of lineations at the margins and the magnetic strain patterns from east to west, all provide the evidences for the occurrence of transpressional tectonics in the region during the emplacement of pluton. The Pasupugallu Gabbro Pluton might have been emplaced into a crustal weak zone developed by the transpressional kinematics along the Terrane Boundary Shear Zone that occurs between the Eastern Ghats Mobile Belt and the East Dharwar craton.

Acknowledgements

The results are a part of a DST-Sponsored Project (ESS/16/189/2003). The authors are thankful to Dr. V.P. Dimri, Director, NGRI, for providing constant encouragement and permission to publish the data. The AMS analysis has been carried out at the Indian Institute of Geomagnetism (IIGM), Alibagh, India and the authors are thankful to the Director, IIGM for his kind cooperation. Helpful suggestions and comments by Dr. Manish Mamtani and anonymous reviewer have helped in substantially improving the manuscript. The authors are grateful to Prof. Somnath Dasgupta for his invitation to contribute this paper. The first author thanks CSIR, New Delhi for providing Senior Research Fellowship.

References

Archanjo, C.J., Bouchez, J.L., Corsini, M., Vauchez, A., 1994. The Pombal granite pluton: magnetic fabric, emplacement and relationships with the Brasiliano strike–slip setting of NE Brazil (Paraiba State). J. Struct. Geol. 16, 323–335.

Archanjo, C.J., da Silva, E.R., Caby, R., 1999. Magnetic fabric and emplacement in a transpressive shear zone system: the Itaporanga porphyritic granite pluton (northeast Brazil). Tectonophysics 312, 331–345.

Asrat, A., Gleizes, G., Barbey, P., Ayalew, D., 2003. Magma emplacement and mafic–felsic magma hybridization: structural evidence from the Pan-African Negash pluton, Northern Ethiopia. J. Struct. Geol. 25, 1451–1469.

Bolle, O., Diot, H., Duchesne, J.C., 2000. Magnetic fabric and deformation in charnockitic igneous rocks of the Bjerkreim–Sokndal layered intrusion (Rogaland, Southwest Norway). J. Struct. Geol. 22, 647–667.

Borradaile, G.J., 1988. Magnetic susceptibility, petrofabrics and strain. Tectonophysics 156, 1–20.

Borradaile, G.J., 2001. Magnetic fabrics and petrofabrics: their orientation distributions and anisotropies. J. Struct. Geol. 23, 1581–1596.

Borradaile, G.J., Henry, B., 1997. Tectonic applications of magnetic susceptibility and its anisotropy. Earth Sci. Rev. 42, 49–93.

Borradaile, G.J., Lagroix, F., King, D., 1998. Tilting and transpression of an Archean anorthosite in northern Ontario. Tectonophysics 293, 239–254.

Brown, M., Solar, G.S., 1998. Shear zone systems and melts: feedback relations and self-organization in orogenic belts. J. Struct. Geol. 20, 211–227.

Cawthorn, R.G. (Ed.), 1996. Layered Intrusions, Developments in Petrology, vol. 15. Elsevier, Amsterdam, p. 531.

Chetty, T.R.K., Murthy, D.S.N., 1994. Collision tectonics in the Eastern Ghats Mobile Belt: mesoscopic to satellite scale structural observations. Terra Nova 6, 72–81.

Cowan, E.J., 1999. Magnetic fabric constraints on the initial geometry of the Sudbury Igneous complex: a folded sheet or a basin-shaped igneous body? Tectonophysics 307, 135–162.

Cruden, A.R., 1998. On the emplacement of tabular granites. J. Geol. Soc. Lond. 155, 853–862.

Dasgupta, S., Sengupta, P., 2003. Indo-Antarctic correlation: a perspective from the Eastern Ghats Granulite Belt, India. Geol. Soc. Lond. Spl. Publ. 206, 131–143.

Day, R., Fuller, M., Schmidt, V.A., 1976. Magnetic hysteresis properties of synthetic titanomagnetites. J. Geophy. Res. 81, 873–880.

Diot, H., Bolle, O., Lambert, J.M., Launeau, P., Duchesne, J.C., 2003. The Tellnes ilmenite deposit (Rogaland, South Norway): magnetic and petrofabric evidence for emplacement of a Ti-enriched noritic crystal mush in a fracture zone. J. Struct. Geol. 25, 481–501.

Dobmeier, C., Raith, M.M., 2003. Crustal architecture and evolution of the Eastern Ghats Belt and adjacent regions of India. In: Yoshida, M., Windley, B.F., Dasgupta, S. (Eds.), Proterozoic East Gondwana: Supercontinent Assembly and Breakup, 206. Geol. Soc. Lond. Spl. Publ., pp. 145–168.

Dunlop, D.J., 1986. Hysteresis properties of magnetite and their dependence on particle size; a test of pseudo single domain remanance model. J. Geophy. Res. 23, 2815–2818.

Ellwood, B.B., Whitney, J.A., 1980. Magnetic fabrics of the Elberton granite, NE Georgia. J. Geophys. Res. 85, 1481–1486.

Ferre, E.C., 2002. Theoretical model of intermediate and inverse AMS fabrics. Geophys. Res. Lett., 29, 7, 10, 1029/2001GL04367.

Gleizes, G., Nedelec, A., Bouhez, J.L., Autran, A., Rochette, P., 1993. Magnetic susceptibility of the Mont-Louis Andorra ilmenite type granite (Pyrenees): a new tool for the petrofabric characterization and regional mapping of zoned granite pluton. J. Geophys. Res. 98, 4317–4331.

Hargraves, R.B., Johnson, D., Chan, C.Y., 1991. Distribution anisotropy: the cause of AMS in igneous rocks? Geophys. Res. Lett. 18, 2193–2196.

Hippertt, J.F., 1994. Structures indicative of helicoidal flow in a migmatitic diapir (Bacao Complex, southeastern Brazil). Tectonophysics 234, 169–196.

Hrouda, F., 2002. The use of the anisotropy of magnetic remanence in the resolution of the anisotropy of magnetic susceptibility in to its ferromagnetic and paramagnetic components. Tectonophysics 347, 269–281.

Jelinek, V., 1981. Characterization of the magnetic fabric of rocks. Tectonophysics 79, T63–T67.

Khan, M.A., 1962. The anisotropy of magnetic susceptibility of some igneous and metamorphic rocks. J. Geophys. Res. 67, 2873–2885.

King, R.F., 1966. The magnetic fabric of some Irish granites. J. Geol. 5, 43–46.

Leelanandam, C., 1989. The Prakasam alkaline province in Andhra Pradesh, India. J. Geol. Soc. India 34, 25–45.

Leelanandam, C., 1990. The Kandra volcanics in Andhra Pradesh: a possible ophiolite. Curr. Sci. 59, 785–788.

Leelanandam, C., Burke, K., Ashwal, L.D., Webb, S.J., 2006. Proterozoic mountain building in Peninsular India: an analysis based primarily on alkaline rock distribution. Geol. Mag. 143 (2), 195–212.

Mezger, K., Cosca, M., 1999. The thermal history of the Eastern Ghats Belt (India), as revealed by U–Pb and 40Ar/39Ar dating of metamorphic and magmatic minerals: implications for the SWEAT hypothesis. Precambrian Res. 94, 251–271.

Nagaraju, J., Chetty, T.R.K., 2005. Emplacement History of Pasupugallu Gabbro Pluton, Eastern Ghats Belt, India: a Structural Study. Gondwana Res. 8, 87–100.

Parada, M.A., Roperch, P., Guiresse, C., Ramírez, E., 2005. Magnetic fabrics and compositional evidence for the construction of the Caleu pluton by multiple injections, Coastal Range of central Chile. Tectonophysics 399, 399–420.

Patterson, S.R., Fowler Jr., T.K., 1993. Re-examining pluton emplacement processes. J. Struct. Geol. 15, 191–206.

Prasada Rao, A.D., Rao, K.N., Murthy, Y.G.K., 1988. Gabbro-anorthosite-pyroxenite complexes and alkaline rocks of Chimakurthy-Elchuru area, Prakasham District, Andhra Pradesh, India. Rec. Geol. Surv. India 116, 1–20.

Ramam, P.K., Murthy, V.N., 1997. Geology of Andhra Pradesh. Geol. Soc. India, Bangalore.

Rochette, P., 1987. Magnetic susceptibility of the rock matrix related to magnetic fabric studies. J. Struct. Geol. 9, 1015–1020.

Rochette, P., Jackson, M., Aubourg, C., 1992. Rock magnetism and the interpretation of anisotropy of magnetic susceptibility. Rev. Geophys. 30, 209–226.

Saint Blanquat, M., Tikoff, B., Teyssier, C., Vigneresse, J.L., 1998. Transpressional kinematics and magmatic arcs. In: Holdsworth, R.E., Strachan, R.A., Dewey, J.F. (Eds.), Continental Transpressional and Transtensional Tectonics, 135. Geol. Soc. Lond. Spl. Publ., pp. 327–340.

Sarkar, A., Paul, D., 1998. Geochronology of the Eastern Ghats Precambrian Mobile Belt—a review. Geol. Surv. India Spl. Publ. 44, 51–86.

Saha, D., 2004. Structural asymmetry and plate tectonic set-up for a Proterozoic fold- and thrust-belt: Nallamalai Fold Belt and adjoining terrane, south India. Geol. Surv. India Spl. Publ. 84, 101–119.

Sengupta, P., Bhattacharya, S., Hamamoto, T., Kagami, H., Yoshida, M., 2001. Tectonic imprints in a suite of granulite-amphibolite facies rocks in and around Chimakurthy, Andhra Pradesh: constrains on the time and amalgamation of the Eaten Ghats Belt and Dharwar Craton. Gondwana Res. 4 (4), 777–778.

Singh, A.P., Mishra, D.C., 2002. Tectono-sedimentary evolution of Cuddapah Basin and Eastern Ghats Mobile Belt (India) as Proterozoic collision: gravity, seismic and geodynamic constraints. J. Geodyn. 33, 249–267.

Symons, D.T.A., 1967. The magnetic and petrologic properties of a basalt column. Geophys. J. R. Astrom. Soc. 12, 473–490.

Tarling, D.H., Hrouda, F., 1993. The Magnetic Anisotropy of Rocks. Chapman and Hall, London, p. 217.

Upadhyay, D., Raith, M.M., Mezger, K., Hammerschmidt, K., 2006. Mesoproterozoic rift–related alkaline magmatism at Elchuru, Prakasam Alkaline province, SE India. Lithos 89, 447–477.

Wing-Fatt, L., Stacey, F.D., 1966. Magnetic anisotropy of laboratory materials in which magma flow is simulated. Pure Appl. Geophys. 64, 78–80.